CrystEngComm

Accepted Manuscript

ROYAL SOCIETY OF CHEMISTRY

www.rsc.org/crystengcomm

For the theme issue of CEC on Functional Co-crystals

Modulating the solubility of Sulfacetamide by means of cocrystals†

N. Rajesh Goud, Ronaq Ali Khan, and Ashwini Nangia*
School of Chemistry, University of Hyderabad, Prof. C. R. Rao Road, Gachibowli, Central University P.O., Hyderabad 500 046, India
ashwini.nangia@gmail.com

Abstract
Sulfacetamide is a popular antibiotic prescribed for treating ocular infections. However various physiological constraints are known to reduce its concentration at the site of action, thereby limiting its therapeutic efficacy. In this crystal engineering study, we report novel cocrystals of sulfacetamide with the objective to lower the solubility of the reference drug and improve its residence time at the site of action. Standard cocrystallization methods resulted in cocrystals with caffeine, isonicotinamide, theophylline, bipyridine and a salt with 4-aminopyridine. These crystalline forms were characterized by thermal, spectroscopic and diffraction techniques. In pH 7 phosphate buffer medium, sulfacetamide–caffeine cocrystal exhibited lower solubility (8.64 g/L, 0.69 times) than the drug (12.5 g/L). The dissolution of sulfacetamide–isonicotinamide and sulfacetamide–caffeine is 0.64 and 0.68 times lower, whereas sulfacetamide–theophylline is comparable to the reference drug. This study highlights a less explored application of pharmaceutical cocrystals to reduce the solubility and dissolution rate of the drug for improved therapeutic action.

† Electronic Supplementary Information (ESI) is available with this paper. HPLC plots of SACT and coformers (Fig. S1), List of compounds used for cocrystal formation (Table S1), Sulfacetamide degradation product (Scheme S1), PXRD of cocrystals (Fig. S2), IR and Raman spectra (Fig. S3 and S4), IR, Raman and ss-NMR peak values (Table S2, S3 and S4), PXRD plots of post solubility/dissolution experiments (Fig. S5). Crystallographic .cif files are downloadable from www.ccdc.cam.ac.uk (CCDC Nos. 981352 – 981356).

For the theme issue of CEC on Functional Co-crystals

Introduction

Sulfacetamide (SACT, hereafter) belongs to the class of sulfonamide antibiotics. It is a frontline drug for the treatment of various ocular infections like trachoma, blepheritis, conjunctivitis and corneal ulcer.[1] It has been investigated as a therapeutic agent for the treatment of pityriasis versicolor and rosacea.[2] Recent reports indicate that it may also act as an antifungal drug by a CYP51A1-independent mechanism.[3] It is a bacteriostatic agent with similar activity against both gram-positive and gram-negative bacteria. SACT has a high solubility of 12.5 g/L.[4] However the therapeutic efficacy of SACT in treating eye infections is severely limited by physiological constraints such as tear flow and reflex blinking which results in considerable drug loss. Such a washout rate reduces the concentration of the drug to one-tenth of its starting value in 4-20 min after administration.[5] As a result only a few percent of the drug dose is absorbed by the eye and therefore the duration of the therapeutic action is very short. This necessitates frequent administration of doses for maintaining optimal therapeutic levels of the drug, which is often inconvenient to patients and also amounts to excess drug loading.

`Remington's[6] pharmacy reference suggests that preparing a less soluble form of a high solubility drug is a convenient method for producing extended release dosage forms. Numerous groups have evaluated extended release systems such as bioadhesive microspheres[5a] and polymeric nanosuspensions[5b] to overcome the limitations of SACT and improve its residence time and therapeutic efficacy at the site of action. Nonetheless, these modifications were not suitable for potential marketing. Entrapment of the drug in a polymeric matrix resulted in poor bioavailability of the drug.[5b] Pharmaceutical cocrystallization,[7] a process by which a drug molecule and a GRAS coformer (generally regarded as safe)[8] are brought together into a single crystal lattice is now an established method to prepare novel solid-state forms of API's with tailored physico-chemical properties. The Cambridge Structural Database (CSD, ver. 5.34, November 2013 update) contains sodium and silver salts of SACT,[9a,b] a cocrystal with caffeine,[9c] and our recent report on polymorphic cocrystals with acetamide.[9d] These solid forms were not investigated for their potential application in addressing excessive elimination issues of the drug. We hypothesized that the hydrogen bonding synthons in the crystal structure of sulfacetamide (CSD refcode SLFNMG01)[9e] could be modified in a graded manner, i.e. the weaker hydrogen bonding interactions in its crystal structure are replaced with stronger hydrogen bonds and better crystal packing with coformers to obtain stable cocrystals. In turn these cocrystals may be useful to lower the solubility of the parent drug. These novel cocrystals were tested in vitro for their potential to lower the solubility and dissolution rate of the drug, altering its half life, and improved bioavailability of SACT, akin to a slow release formulation.[10] A recent report on the pharmaceutical cocrystals of epigallocatechin-3-gallate (EGCg)[11] lends credence to our hypothesis. Zaworotko and coworkers[11] showed that cocrystals of EGCg exhibited lower solubility compared to the parent drug resulting in significant alteration in the pharmacokinetic profile and improved bioavailability. Similar implications were echoed by Higuchi and Pitman[12] almost four decades ago on the oral bioavailability of caffeine in low-solubility complexes with gentisic acid. Mechanochemical grinding,[13] slurry grinding and solution crystallization

techniques were used to screen SACT with various GRAS coformers which resulted in novel cocrystals with theophylline (THEO), isonicotinamide (INIC), caffeine (CAF), bipyridine (BIP) and a salt with 4-aminopyridine (4AP) (Scheme 1). The crystallization, characterization, solubility and dissolution rate of SACT cocrystals are discussed in this article.

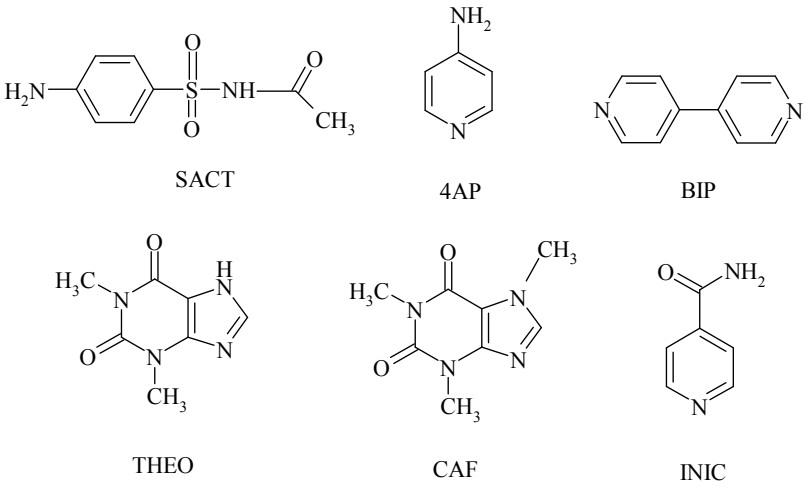

Scheme 1 Sulfacetamide and coformers in this study. Compound abbreviations are used throughout the paper.

Experimental Section

SACT and coformers (purity > 99.8%) were purchased from Sigma-Aldrich (Hyderabad, India). Solvents (purity > 99%) were purchased from Hychem Laboratories (Hyderabad, India) for crystallization experiments. Water and solvents (HPLC grade) were purchased from Merck Chemicals (Bangalore, India) for solubility and dissolution experiments.

Preparation of SACT cocrystals

SACT-BIP cocrystal SACT (214.2 mg) and 4,4'-BIP (78.0 mg) in 1:0.5 molar ratio were slurry ground in 5 mL of EtOH for 8 h. The formation of cocrystal was confirmed by PXRD and DSC. 30 mg of this material was dissolved in 5 mL EtOH and left for slow evaporation at ambient conditions. Single crystals suitable for X-ray diffraction were obtained after 3-4 days. The same cocrystal was also obtained on manual grinding of SACT and BIP in 1:0.5 stoichiometric ratio for 30 min.

SACT-CAF cocrystal SACT (214.2 mg) and CAF (194.2 mg) in 1:1 molar ratio were slurry ground in 4 mL of EtOH for 24 h. The formation of cocrystal was confirmed by PXRD and DSC. 30 mg of this material was dissolved in 5 mL EtOH and left for slow evaporation at ambient conditions. Single crystals suitable for X-ray diffraction were obtained after 3-4 days. The same cocrystal was also obtained on manual grinding of SACT and CAF in 1:1 stoichiometric ratio for 30 min.

SACT-INIC cocrystal SACT (214.2 mg) and INIC (244.24 mg) in 1:2 molar ratio were slurry ground in 2.5 mL of toluene and 1.5 ml of EtOAc solvent mixture for 24 h. The formation of cocrystal was confirmed by PXRD and DSC. 30 mg of this material was dissolved in 4 mL of

1:1 mixture of toluene and ethyl acetate solvent mixture and left for slow evaporation at ambient conditions. Single crystals suitable for X-ray diffraction were obtained after 4-5 days. The same cocrystal was also obtained on manual grinding of SACT and INIC in 1:2 stoichiometric ratio for 30 min.

SACT-THEO cocrystal SACT (214.2 mg) and THEO (180.2 mg) in 1:1 molar ratio were slurry ground in 4 mL of i-PrOH for 24 h. The formation of cocrystal was confirmed by PXRD and DSC. 30 mg of this material was dissolved in 4 mL of i-PrOH and left for slow evaporation at ambient conditions. Single crystals suitable for X-ray diffraction were obtained after 4-5 days.

SACT-4AP salt SACT (214.2 mg) and 4AP (94.11 mg) in 1:1 molar ratio were manually ground for 30 min. Salt formation was confirmed by PXRD and DSC. 30 mg of this material was dissolved in 4 mL of EtOH and left for slow evaporation at ambient conditions. Single crystals suitable for X-ray diffraction were obtained after 3-4 days.

X-ray crystallography Crystal structures of SACT-CAF, SACT-4AP and SACT-THEO were collected on a Bruker SMART APEX-CCD diffractometer. Mo-Kα (λ = 0.71073 Å) radiation was used to collect X-ray reflections on a single crystal. While data on SACT–CAF and SACT–THEO was collected at 100 K, SACT–4AP was collected at 298 K. Data reduction was performed using Bruker SAINT software.[14a] Intensities for absorption were corrected using SADABS.[14b] Crystal structures were solved by direct methods and refined on F^2 with SHELXS-97 and SHELXL-97 programs to give satisfactory *R* factor.[14c,d] X-ray reflections on SACT-BPN and SACT-INIC cocrystals were collected on an Xcalibur Gemini EOS CCD diffractometer[14e] (Oxford Diffraction, Yarnton, UK) using Mo-Kα, radiation at 298K. Data reduction was performed using CrysAlisPro (version 1.171.33.55). OLEX2-1.0,[14f] and SHELX-TL 97 were used to solve and refine the reflections data. Non hydrogen atoms were refined anisotropically. Hydrogen atoms on O and N were experimentally located in difference electron density maps. All C–H atoms were fixed geometrically using HFIX command in SHELX-TL. A check of the final CIF file using PLATON[14g] did not show any missed symmetry. X-Seed[14h,i] was used to prepare packing diagrams.

Powder X-ray diffraction Powder X-ray diffraction of the samples were recorded on Bruker D8 Focus diffractometer using Cu-Kα X-radiation (λ = 1.5406 Å) at 40 kV and 30 mA. Diffraction patterns were collected over 2θ range of 5-50° at scan rate of 1°/min.

Vibrational spectroscopy Nicolet 6700 FT-IR spectrometer with a NXR FT-Raman and NIR Module was used to record IR and Raman spectra. IR spectra were recorded on samples dispersed in KBr pellets. Raman spectra were recorded on samples contained in standard NMR diameter tubes or on compressed samples contained in a gold-coated sample holder.

Thermal analysis DSC was performed on a Mettler Toledo DSC 822e module. 3-5 mg of sample was used for this characterization. Samples were placed in sealed pin-pricked aluminum pans and characterized at a heating rate of 5°C min^{-1} in the temperature range of 30-250 °C. Samples were purged by a stream of dry nitrogen flowing at 80 mL/min.

Solid-state NMR spectroscopy Solid-state ^{13}C NMR spectra were recorded on Bruker Avance 400 MHz spectrometer (Bruker-Biospin, Karlsruhe, Germany, operating at 100 MHz for ^{13}C

nucleus). ss-NMR measurements were carried out on Bruker 4-mm double resonance CP-MAS probe in zirconia rotors with a Kel-F cap at 5.0 kHz spinning rate with a cross-polarization contact time of 2.5 ms and a delay of 8s. ^{13}C NMR spectra were recorded at 100 MHz and referenced to the methylene carbon of glycine, and then recalibrated to the TMS scale ($\delta_{glycine}$ = 43.3 ppm).

Solubility and dissolution The solubility and dissolution experiments were performed using HPLC method. Prior to estimating solubility and dissolution rates, calibration curves were determined for each compound. Various dilutions of a stock solution of SACT and cocrystals in pH 7 phosphate buffer were made and their respective retention times were determined using HLPC at λ_{max} 254nm (λ_{max} of SACT). By plotting known concentration of each dilution vs. corresponding area, calibration curve for each compound was obtained. HPLC was done on Shimadzu Prominence model LC-20AD equipped with a PDA detector and C-18G column (250 mm x 4.6 mm ID, 5µm particle size and 120Å pore size). Elution was achieved by a mobile phase made of 85:15 ratio of water with 1% acetic acid: Methanol in an isocratic method. The retention times of standard aqueous solutions of SACT, CAF, THEO and INIC were found to be 8.2, 41.4, 22.2 and 3.6 min, respectively and the same were observed even for the cocrystals (Fig S1). SACT has 73.3, 42.3 and 66.4% contribution in SACT–CAF, SACT–INIC and SACT–THEO cocrystals. The quantification of SACT in test solutions obtained from equilibrium solubility and dissolution experiments was done by comparison of the HPLC peak area with that of the standards. Equilibrium solubility was determined in pH 7 phosphate buffer using shake-flask method.[15] Excess amount of powdered material was added to 5 ml of the buffer solution and the resulting suspension was stirred at room temperature for 24hrs. The suspension was filtered through 0.45µ syringe filter and the concentration of the resultant solution determined. Intrinsic dissolution rate (IDR) measurements were carried on a USP-certified Electrolab TDT-08 L dissolution tester by the disk intrinsic dissolution method. For IDR experiments, 500 mg of pure SACT and the cocrystals were taken in the intrinsic attachments and compressed to a 0.5 cm^2 disk using a hydraulic press at a pressure of 2.5 ton/$inch^2$ for 5 min. The intrinsic attachments were placed in jars of 900 mL of pH 7 phosphate buffer preheated to 30°C and rotated at 150 rpm. 5 ml aliquots were collected at specific time intervals, and concentrations of the aliquots were determined with proper dilution from the predetermined calibration curves. The linear region of the dissolution profile (regression > 0.99) was used to determine the IDR of the compound as [slope of the amount dissolved÷ surface area of the pellet] per unit time. There was no transformation of SACT or cocrystals upon tablet compression as confirmed by PXRD.

Results and Discussion

The supramolecular synthon strategy[16] guided by hydrogen bonding rules[17] is the primary design element for the construction of multi-component cocrystals. Based on the nature of the functional groups in a drug molecule, coformers with complementary functional moieties were selected so as to optimize strong and robust synthons.[18] The primary functional groups in SACT are amide and amine moieties. In the literature, COOH, $CONH_2$, N-oxide, pyridine etc. functional moieities

have been reported to assemble with amide containing molecules. Accordingly, SACT was cocrystallized with GRAS coformers containing the above functional groups. A complete list of all the coformers is listed in Table S1, ESI†. Surprisingly, we did not obtain any cocrystals with COOH containing coformers which have 48% probability of heterosynthon formation with the amide functional group,[19] but instead the cocrystals are sustained by hydrogen bonding with the amide and pyridine coformers, which have a CSD probability of 35% and 4% for the respective synthons.[19c] In addition the cocrystals contained multiple molecules in the asymmetric unit and variable stoichiometry: SACT–CAF (1:1), SACT–INIC (1:2), SACT–THEO (2:2), SACT–BIP (1:0.5) and SACT–4AP (1:1). These cocrystals have different Z" (Z" = sum of Z' values in multi-component crystals)[20] in their crystal structures (Table 1). The X-ray crystal structure of SACT–CAF was redetermined with better *R*-factor. Hydrogen bond parameters are listed in Table 2.

Table 1 Crystallographic parameters of SACT cocrystals.

	SACT-BPN (1:0.5)	SACT-CAF (1:1)	SACT-INIC (1:2)	SACT-THEO (2:2)	SACT-4AP (1:1)
Emp form	$C_{13}H_{14}N_3O_3S$	$C_{16}H_{20}N_6O_5S$	$C_{20}H_{22}N_6O_5S$	$C_{15}H_{18}N_6O_5S$	$C_{13}H_{16}N_4O_3S$
Form wt	292.33	408.44	458.50	394.41	308.36
Cryst syst	Monoclinic	Monoclinic	Monoclinic	Triclinic	Monoclinic
Sp gr	$P2_1/n$	$P2_1/c$	$P2_1/n$	$P\bar{1}$	$P2_1/c$
T (K)	298(2)	100(2)	298(2)	100(2)	298(2)
a (Å)	11.6469(9)	7.1821(6)	10.7667(4)	8.6640(7)	7.7413(7)
b (Å)	10.4670(6)	30.430(3)	9.7508(4)	14.9675(13)	17.8726(16)
c (Å)	12.4421(9)	8.8188(7)	21.1014(7)	15.3632(15)	11.0065(10)
α (º)	90	90	90	110.234(2)	90
β (º)	116.510(10)	107.6790(10)	96.176(3)	106.3650(10)	97.8790(10)
γ (º)	90	90	90	97.2830(10)	90
Z	4	4	4	4	4
Z"	1.5	2	3	4	2
V ($Å^3$)	1357.31(17)	1836.3(3)	2202.45(14)	1737.1(3)	1508.5(2)
Cryst density (g/cm^3)	1.431	1.477	1.383	1.508	1.358
Rflns. collect	4882	18761	7836	18179	15456

Unique rflns.	2315	3579	3762	6823	2992
Obsd. rflns.	1910	3358	3002	5929	2698
Parameters	183	269	318	525	211
R_1	0.0404	0.0436	0.0407	0.0505	0.0496
wR_2	0.1131	0.1158	0.1057	0.1297	0.1226
GOF	1.035	1.074	1.065	0.953	1.191

Table 2 Hydrogen bond distances and angles in SACT cocrystals (neutron-normalized N–H 1.009 Å, O–H 0.983 Å, and C–H 1.083 Å distances).

D–H···A	D···A (Å)	H···A (Å)	D–H···A (°)	symmetry code
SACT–BPN (1:0.5)				
N1–H1B···O3	3.008(3)	2.44	124	3/2–x, –1/2+y,1/2–z
N2–H2···N3	2.889(3)	2.10	153	1/2–x, 1/2+y,1/2–z
C2–H2A···O1	2.956(3)	2.60	103	--[a]
C8–H8A···O2	3.399(4)	2.44	178	1/2–x, 1/2+y,1/2–z
SACT–CAF (1:1)				
N1–H1A···N5	2.842(2)	2.12	175	1+x,y,1+z
N2–H2A···O1	2.991(2)	2.18	172	x,y, –1+z
N2–H2B···O5	2.941(3)	2.07	170	1–x, –y, –z
C6–H6···O1	2.936(2)	2.59	102	--[a]
C13–H13···O3	3.197(3)	2.28	163	–1+x,1/2–y, –1/2+z
C15–H15B···O4	2.755(3)	2.29	108	--[a]
SACT–INIC (1:2)				
N1–H1···N3	2.852(2)	2.00	177	1/2–x, –1/2+y,1/2–z
N2–H2A···O3	2.920(3)	2.06	166	–x, –y, –z
N2–H2B···N2	3.109(4)	2.49	131	–x,1–y, –z
N4–H4A···O5	3.092(2)	2.26	169	1–x, –y, –z
N4–H4B···N5	2.982(2)	2.11	179	–1/2+x,1/2–y, –1/2+z
N6–H6A···O4	2.941(3)	2.03	168	1–x,1–y, –z
N6–H6B···O5	2.961(2)	2.15	164	1–x, –y, –z
C8–H8A···O1	3.142(3)	2.48	126	1/2–x, –1/2+y,1/2–z
C10–H10···O5	3.369(3)	2.44	173	1–x, –y, –z
C13–H13···O2	3.299(3)	2.54	139	x,1+y,z
SACT–THEO (2:2)				

N1–H1···N11	2.797(3)	2.00	165	2–x, –y,1–z
N2–H2A···O1	3.026(3)	2.17	171	–1+x,y,z
N2–H2B···O10	2.868(3)	2.04	169	1–x,1–y,1–z
N3–H3A···O5	2.969(3)	2.13	174	1+x,y,z
N3–H3B···O8	2.886(3)	2.07	157	2–x,1–y,1–z
N4–H4···N7	2.812(3)	2.00	163	–1+x,y,z
N8–H8D···O6	2.791(3)	1.95	174	–1+x,y,z
N12–H12A···O3	2.803(3)	1.95	177	1–x, –y,1–z
C2–H2···O2	2.896(3)	2.52	104	--[a]
C8–H8A···O4	3.344(3)	2.51	143	x, –1+y,z
C14–H14···O4	2.943(3)	2.58	103	--[a]
C16–H16A···O4	3.184(3)	2.55	123	1 –x,1 –y, –z
C21–H21···O4	3.137(3)	2.37	137	1 –x,1 –y, –z
C21–H21···O6	3.251(3)	2.43	145	1 –x,1 –y, –z
C22–H22B···O7	2.739(3)	2.30	106	--[a]
C23–H23A···O8	3.316(3)	2.49	142	1 –x,1 –y,1 –z
C28–H28···O2	3.200(2)	2.50	130	x,y,1+z
C28–H28···O3	3.307(3)	2.43	153	x,y,1+z
C29–H29B···O9	2.722(3)	2.37	100	--[a]
C30–H30A···O10	2.761(3)	2.37	103	--[a]
SACT–4AP (1:1)				
N2–H2A···O1	3.146(3)	2.41	153	1–x, –1/2+y,1/2–z
N2–H2B···O2	2.999(4)	2.19	166	x,1/2–y,1/2+z
N3–H3A···N1	2.783(3)	1.87	178	1–x, –1/2+y,1/2–z
N4–H4A···O3	2.806(3)	1.97	164	1+x,y,z
C2–H2···O2	2.914(3)	2.54	105	--[a]
C5–H5···O3	3.337(3)	2.46	157	x,1/2–y,1/2+z

[a] Intramolecular hydrogen bond

Crystal structures

Sulfacetamide–Bipyridine (SACT–BPN) cocrystal This cocrystal structure contains 1 molecule of SACT and half molecule of BPN in the asymmetric unit. SACT molecules are arranged along the 2_1 screw axis connected through N–H···O hydrogen bonds (2.44 Å, 124°). Such screw related helices of SACT molecules are bridged by BPN coformer molecules through a N–H···N interaction (2.10 Å, 153°; Fig. 1a). These H bonds extend the SACT and BPN molecules in a 2D arrangement, with a C–H···O interaction connecting the layers (Fig. 1b and 1c). The hydrogen bonds in this and subsequent crystal structure are generally weaker/ longer

than standard N–H···O/ O–H···O hydrogen bond distances but comparable to the previous study on the same system.[9d]

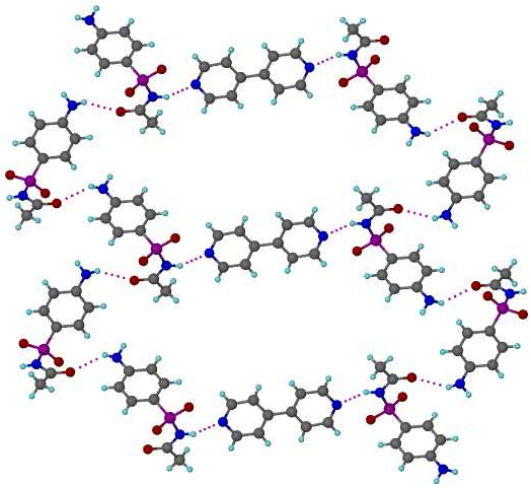

Fig. 1a Screw-axis related SACT molecules are bridged by BPN molecules.

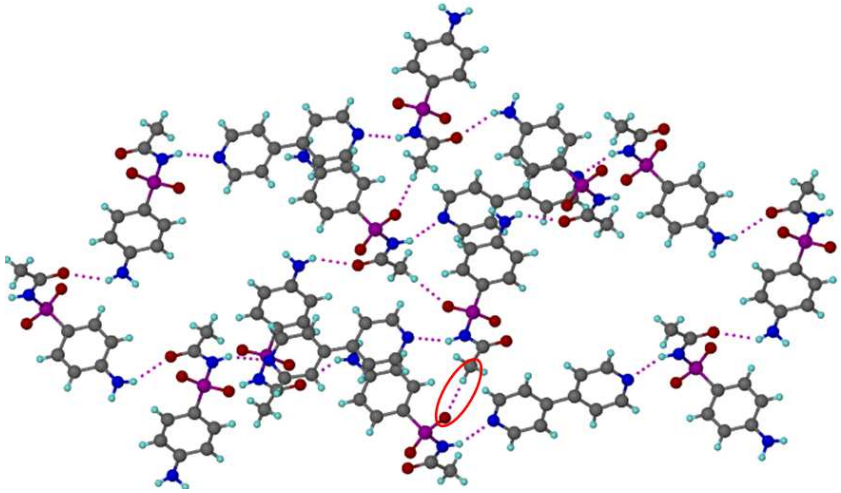

Fig. 1b Adjacent layers connected through C–H···O interactions (highlighted by a circle, top view).

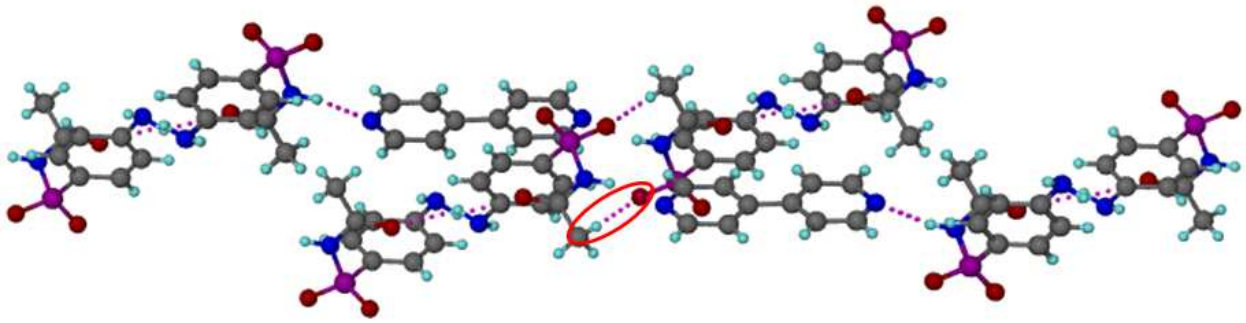

Fig. 1c Adjacent layers connected through C–H···O interactions (highlighted by a circle, side view).

Sulfacetamide–Caffeine (SACT–CAF) cocrystal This 1:1 stoichiometric cocrystal was obtained by slow evaporation from EtOH. SACT molecules are connected in a chain along the *c*-axis through N–H···O hydrogen bond (2.18 Å, 172°). Adjacent layers of SACT molecules are bridged by two CAF molecules connecting through N–H···O and N–H···N H-bonds (2.07 Å, 170°; 2.12 Å, 175°; Fig. 2a). Such discrete units are connected through C–H···O interactions (2.28 Å, 163°; Fig. 2b).

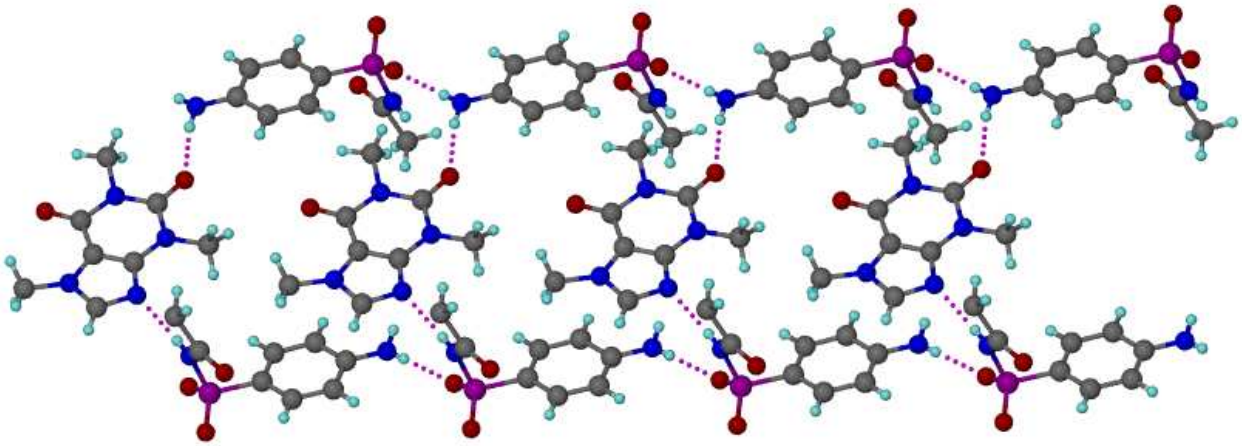

Fig. 2a Linear chains of SACT molecules bridged through CAF coformer molecules (only one layer of CAF molecules is shown for clarity).

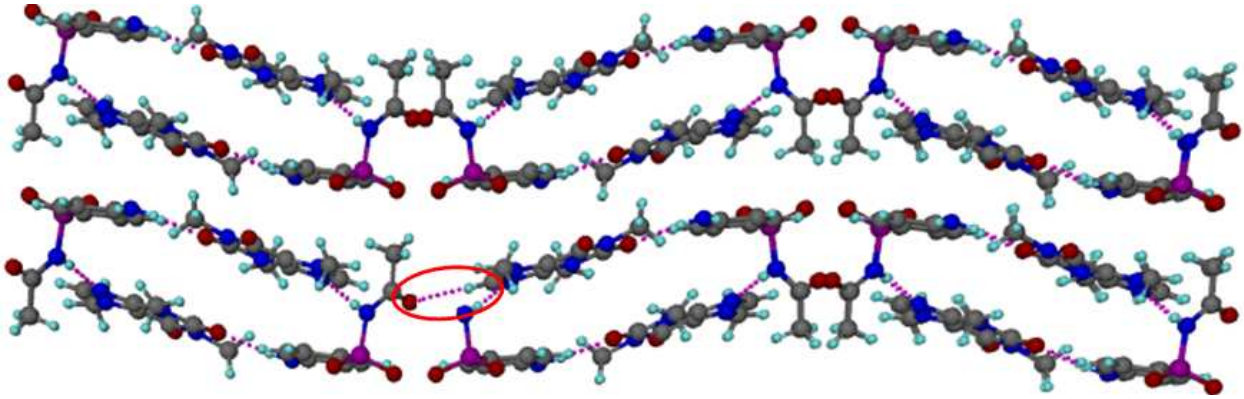

Fig. 2b Discrete units of SACT and CAF molecules are connected through C–H···O hydrogen bonds (marked by a circle). The CH_3CO– group of SACT which blocks the C–H···O hydrogen bond (marked by a circle) is deleted for clarity.

Sulfacetamide–Isonicotinamide (SACT–INIC) cocrystal Initially, single crystals of this 1:2 cocrystal were obtained on crystallizing 1:1 molar ratio of SACT and INIC along with a few crystals of SACT from toluene–ethyl acetate solvent mixture. The stoichiometry was optimized by crystallizing SACT and INIC in 1:2 ratio which resulted in complete conversion of the starting materials to the cocrystal. The crystal structure could well have had the expected 1:1 stoichiometry. It is as though the second molecule of INIC resides in the crystal structure as a

linear spacer dimer connecting the SACT–INIC units (symmetry independent INIC molecules are shaded differently). Unlike previous structures, SACT molecules in this cocrystal form a dimer like discrete unit (2.11 Å, 179°) which are connected through a INIC dimer (N–H···O hydrogen bond (2.06 Å, 166°, 2.15 Å, 164°). SACT molecules self-assemble through a $R^2_2(8)$ ring motif[21] (2.06 Å, 166°; Fig. 3a). Such 1D units of SACT and INIC are connected through a N–H···O (2.03 Å, 168°; Fig. 3b) hydrogen bond.

Fig. 3a SACT molecules are connected through INIC coformers. The crystallographically nonequivalent INIC molecules are distinguished by cap-stick and ball-stick models.

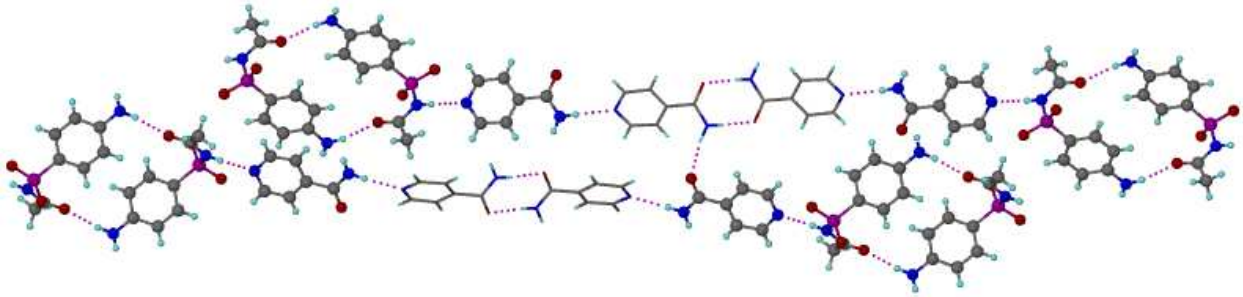

Fig. 3b N–H···O hydrogen bond connects the 1D units of SACT and INIC.

Sulfacetamide-Theophylline (SACT-THEO) cocrystal This equimolar stoichiometry cocrystal was obtained when SACT and THEO in 1:1 ratio were dissolved in i-PrOH and left for evaporation. SACT molecules extend as a chain along the *a*-axis through N–H···O H bond in each pair (2.13 Å, 174°; 2.17 Å, 171°). Adjacent chains of SACT molecules are connected by THEO molecules through N–H···O and N–H···N H bonds (Fig. 4). The crystallographically nonequivalent pairs of SACT and THEO molecules behave as distinct entities of 1:1 cocrystal domains are connected through a C–H···O interaction (2.51 Å, 143°).

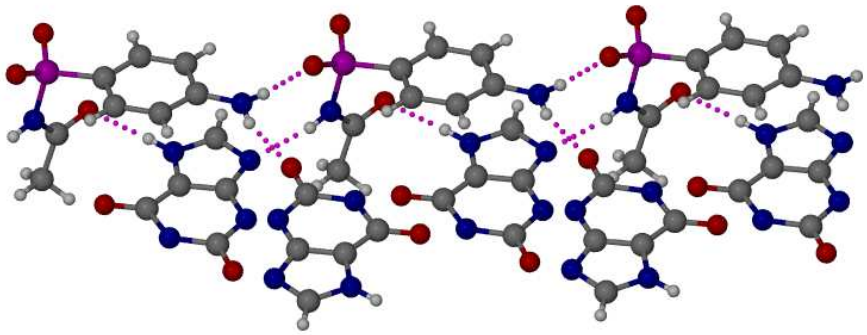

Fig. 4a Linear chain of SACT molecules are bound through THEO coformer molecules. The methyl groups of THEO molecules are deleted for clarity.

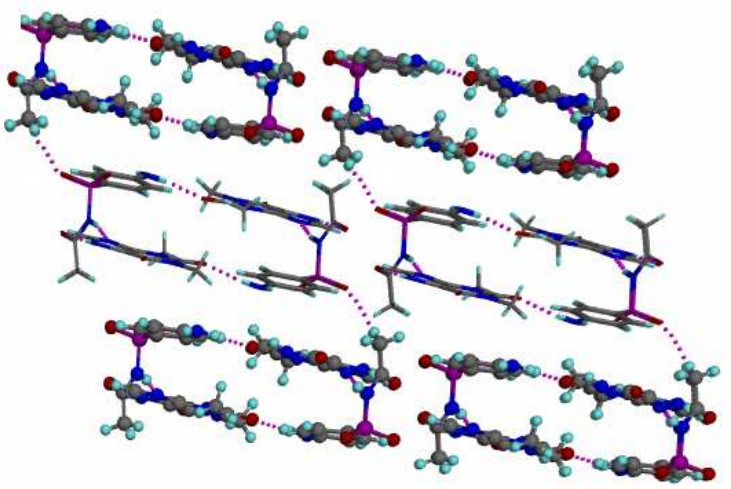

Fig. 4b Discrete pairs of SACT and THEO molecules are connected through a C–H···O interaction.

Sulfacetamide-4-amino pyridine (SACT-4AP) salt Solution crystallization of SACT and 4AP in 1:1 stoichiometry resulted in a salt with proton transfer from the amide N–H of SACT to the pyridyl nitrogen of 4AP. The amide nitrogen is sandwiched between the electron-withdrawing carbonyl and sulfonyl groups and is acidic enough with a pKa of 4.3 to transfer its proton to the basic nitrogen of 4AP (pK_a = 8.95). The ΔpKa value (ΔpKa = 4.65) is in the normal proton transfer range according to the 'rule of three'.[22] Screw related SACT molecules are bonded by N–H···O (2.19 Å, 166°) H bonds which are connected to 4AP by N–H···N^- (1.87 Å, 178°) and N–H···O (1.97 Å, 164°) H bonds (Fig. 5).

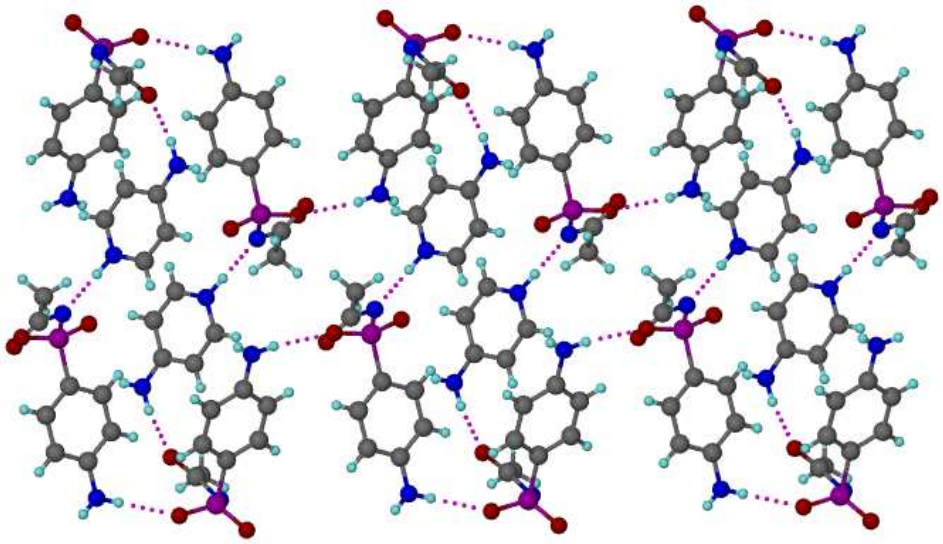

Fig. 5 SACT molecules are connected by 4AP through N–H···O and N–H···N^- H bonds.

For the theme issue of CEC on Functional Co-crystals

Thermal analysis

DSC analyses of SACT cocrystals showed unique thermal behavior in comparison to their starting materials (Fig. 6). The purity of all the cocrystals was indicated by a single, sharp melting endotherm in DSC. Unlike reported cocrystal case studies,[7a,23] we did not observe a correlation between the melting points of SACT cocrystals with those of the coformers (Table 3). In the DSC thermogram of SACT, SACT−CAF and SACT−THEO, an extra decomposition hump after the usual melting endotherm was observed due to the degradation of SACT to sulfanilamide and acetic acid (Scheme S1) at high temperature.[6,24] The observed decomposition peak in the thermograms is probably due to this degradation.

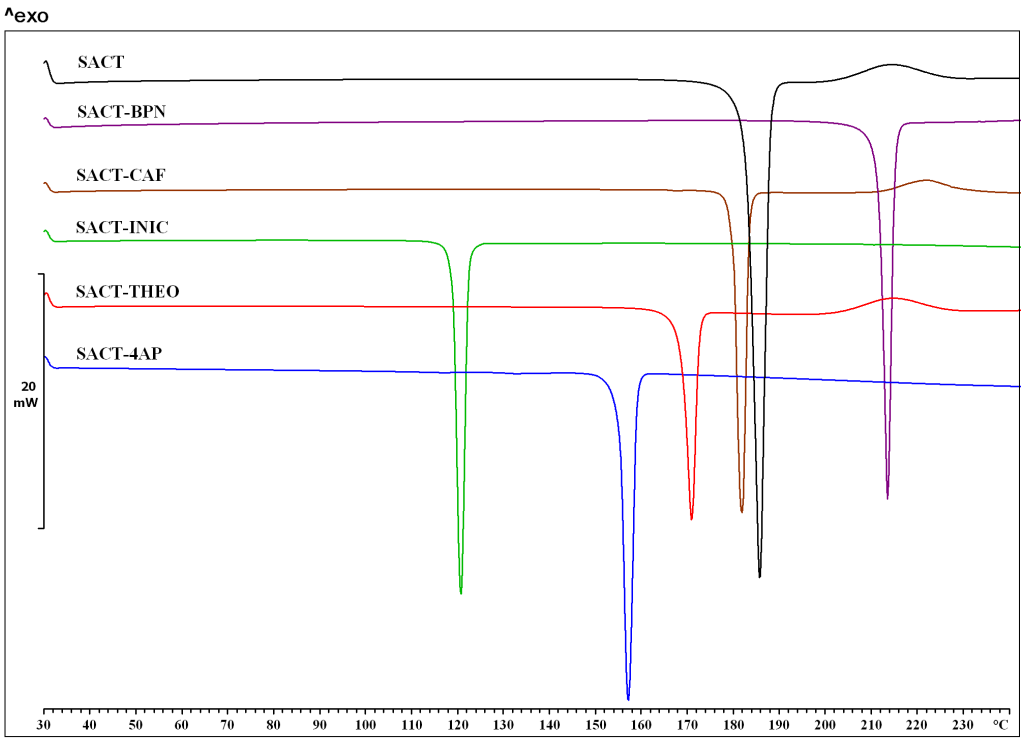

Fig. 6 Heating curves of SACT cocrystals depicting their unique melting behavior.

Table 3 Melting points of SACT[a] salt/cocrystals and the coformers.

S. No	SACT cocrystal/salt	Melting Point (°C)	Coformer	Melting Point (°C)
1	SACT−BPN	211-213	4,4'-Bipyridine	110-114
2	SACT−CAF	179-181	Caffeine	238-240
3	SACT−INIC	119-121	Isonicotinamide	155-157
4	SACT−THEO	169-171	Theophylline	272-274

5	SACT−4AP	156-158	4-aminopyridine	155-156

[a] The m.p. of SACT is 183-185 °C.

Powder X-ray diffraction

Powder diffraction is a reliable technique to establish the unique diffraction patterns of a novel solid form in comparison to the starting materials.[25a] It is the method of choice for those cases where single crystals are not available by crystallization. Its application has been diversified with the detection of polymorphic impurity in a mixture of polymorphs, bulk purity of polymorphs, cocrystals or salts, amorphous content in a crystalline material and structure solution of a crystalline material from powder diffraction data.[25] PXRD was used to establish the bulk purity of SACT cocrystals. The experimental powder patterns of bulk materials of cocrystals showed excellent match when stacked with their calculated patterns (Fig. S2).

Vibrational Spectroscopy

The nature of hydrogen bonding and the extent of ionization can invariably influence the vibrational energy levels of compounds on forming cocrystals or salts. IR and Raman spectra are sensitive to such changes, being able to identify and distinguish novel solid forms from their starting components.[26a] In the IR spectrum of SACT, the N–H asymmetric and symmetric stretching frequencies appeared at 3471.2, 3380.7 and 3257.0 cm^{-1}. The amide carbonyl stretch was observed at 1685.7 cm^{-1} and the N-H bending mode at 1596.4 cm^{-1}. Significant changes in these vibrational modes were observed upon the formation of cocrystal/ salt (Fig. S3). In SACT−BPN cocrystal, the N−H stretching modes shifted to 3475.6, 3375.3 cm^{-1}. While the N−H bending modes moved to 1594.0 cm^{-1}, the amide –C=O stretch appeared at 1704.1cm^{-1}. On forming cocrystal, the C=N stretch of BPN shifted from 1407.3 cm^{-1} to 1409.9 cm^{-1}. Similar differences were also observed in the stretching and bending modes of other cocrystals. While the N−H stretching frequencies appeared at 3441.7, 3358.1 and 3255.8 cm^{-1} in SACT-−CAF, they showed up at 3428.4, 3396.6, 3345.9 and 3239.2 cm^{-1} in SACT−INIC and 3471.3 and 3380.8 cm^{-1} in SACT-THEO. The corresponding carboxamide C=O stretch was observed at 1702.0 and 1658.7 cm^{-1} in SACT-CAF, 1697.2 and 1674.2 cm^{-1} in SACT−INIC, and 1716.1, 1667.8 cm^{-1} in SACT−THEO. Larger shifts in the N−H stretching frequencies were observed in the case of SACT-4AP where proton transfer from amide N−H to pyridyl nitrogen resulted in salt. The N-H stretching frequencies here were observed at 3444.4, 3422.9, 3350.3 and 3242.0 cm^{-1} and the carboxamide –C=O stretch at 1656.2 cm^{-1}. Major FT-IR vibrational frequencies of SACT cocrystals are shown in Table S2.

The complementary Raman spectra[26b] where the symmetric stretching frequencies have stronger intensities compared to the asymmetric modes, showed significant shifts in the Raman intensities on forming the product cocrystal/ salt. The Raman intensities for asymmetric and symmetric N−H and C=O stretching frequencies appeared at 3479.5, 3380.7 and 1688.0 cm^{-1} respectively. These peak positions showed significant shift in the cocrystals/salt. While the N-H asymmetric and symmetric intensities appeared at 3475.5, 3377.1 in SACT–BPN, 3443.3,

3358.2, 3256.3 in SACT-CAF, 3472.4, 3381.6 cm^{-1} in SACT–THEO and 3445.2, 3426.4, 3354.2, 3243.8 cm^{-1} in SACT–4AP the corresponding –C=O stretch was observed at 1707.1 cm^{-1} in SACT–BPN, 1703.4 cm^{-1} in SACT–CAF, 1699.7 cm^{-1} in SACT–INIC, 1708.3 cm^{-1} in SACT–THEO (Fig. S4). The important FT-Raman peaks are shown in Table S3.

Solid state NMR spectroscopy

ss-NMR is gaining importance as a routine technique for characterizing pharmaceutical solids because of its sensitivity to changes in hydrogen bonding interactions and molecular conformation.[27] It is a non-destructive method necessitating minimum amount of sample for characterization. ^{13}C ss-NMR of SACT cocrystals showed significant differences in chemical shifts in comparison to their individual components. The C=O carbon of SACT appeared at δ 171.8 ppm, whereas this peak appeared at 170.7 ppm in SACT-BPN, 171.2 ppm in SACT-CAF, 170.5 ppm in SACT-INIC, 171.3 ppm in SACT-THEO and 170.9 ppm in SACT-4AP due to changes in hydrogen bonding and local environment. The remaining carbon nuclei appear at different chemical shifts to distinguish from the starting components (Fig. 7, Table S4).

For the theme issue of CEC on Functional Co-crystals

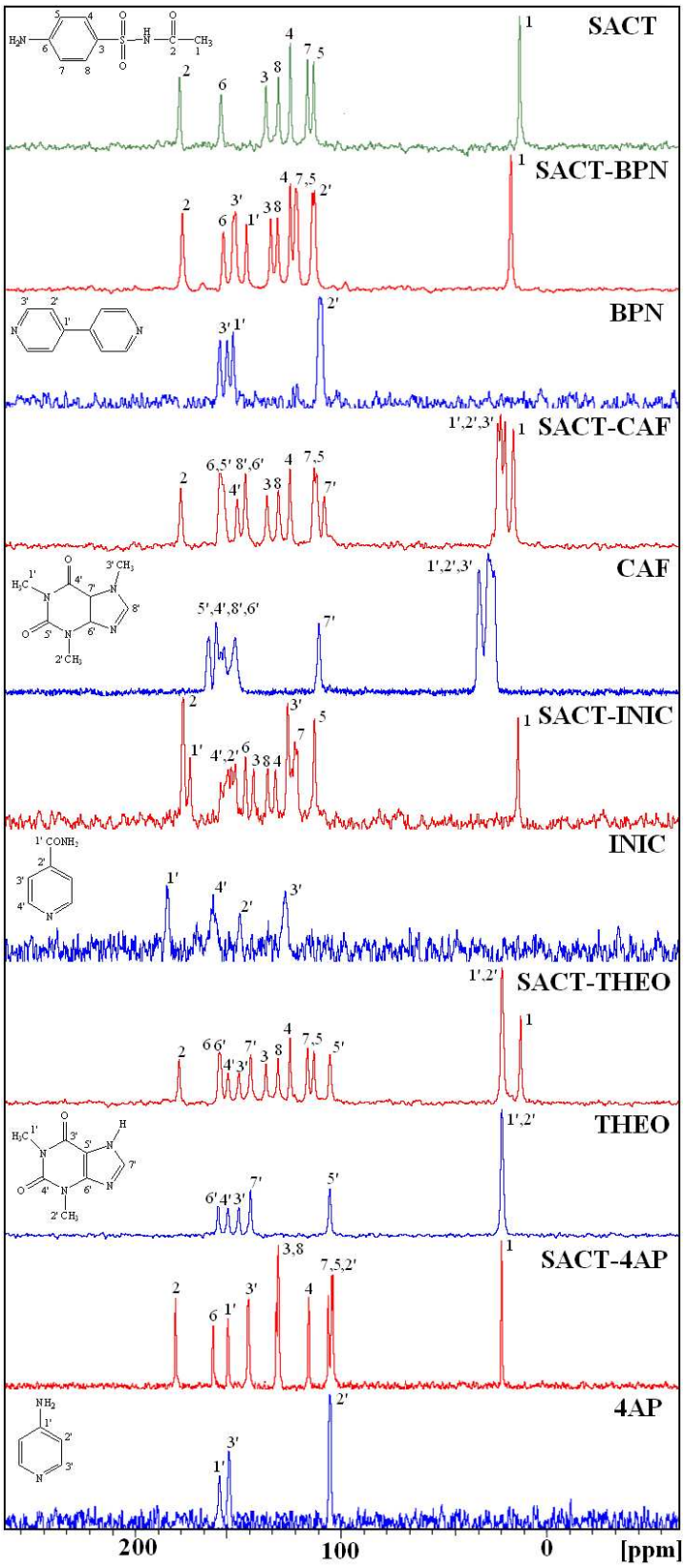

Fig. 7 Overlay of 13C ss-NMR spectra of SACT cocrystals with the individual components.

Solubility and Dissolution

The primary objective of developing cocrystals of SACT was to address the poor residence time of the drug at the site of action due to its rapid elimination. We reasoned that modulating the hydrogen bonding in the parent drug structure with appropriate coformers would result in cocrystals with stronger hydrogen bond synthons and better crystal packing, and the stable crystal lattice would lower the solubility of SACT and prolong its residence time at the ocular surface. In terms of crystal density, which is a good indicator of molecular packing in the crystal lattice, the density of SACT cocrystals is higher than that of sulfacetamide (1.377 g/cm^3). Given the high aqueous solubility of 12.5 g/L for sulfacetamide,[4] solubility and dissolution experiments on SACT cocrystals were performed in pH 7 phosphate buffer medium and the samples were analyzed by HPLC using a PDA detector. Equilibrium solubility experiments were performed for 24 h by making a supersaturated solution of SACT cocrystals in phosphate buffer medium at pH 7. These experiments showed that SACT−CAF is stable to the equilibrium solubility conditions over 24 h, but SACT−INIC and SACT−THEO are less stable and dissociated to their individual components and precipitated SACT out of solution. The solubility of stable SACT−CAF cocrystal is 8.64 g/L (0.7 times) compared to that of SACT at 12.5 g/L, indicating that the thermodynamic solubility of SACT can be lowered by forming a cocrystal with caffeine.

Due to the dissociation of SACT cocrystals in equilibrium solubility measurements, dissolution experiment (a kinetic method) was adopted to determine the rate at which the drug dissolves in solution. The intrinsic dissolution rate (IDR) is particularly useful in determining the solubility of metastable forms before they convert to the more stable polymorph/ hydrate etc. IDR experiments on SACT cocrystals were performed in pH 7 phosphate buffer media for 4 h by the rotating disk intrinsic dissolution rate (DIDR) method[28] at 30°C (Fig. 8, Table 4). SACT–INIC showed 0.64 times the IDR of SACT followed by SACT–CAF (x0.68) and SACT–THEO (x1). SACT and SACT–CAF were stable at the end of the dissolution experiment, but SACT–INIC and SACT–THEO cocrystals dissociated into their individual components precipitating the parent drug. The low solubility and dissolution of cocrystals may be rationalized based on their stronger hydrogen bonding interactions and better packing efficiency as compared to SACT. The molecules extend through intermolecular N–H···O hydrogen bonds supported by a single auxiliary C–H···O interaction in the crystal structure of sulfacetamide (see refcode SLFNMG01 in the CSD) However in case of cocrystals the molecules propagate through stronger N–H···O and N–H···N bonds further stabilized by C–H···O interactions (Table 2). Thus the cocrystals exhibit better packing efficiency and stronger crystal lattice which has lower solubility and dissolution compared to SACT. The solubility of drugs has been controlled by cocrystals.[11,12,29] We did not find any correlation between the melting point of the cocrystal and its solubility.[7a] PXRD plots of the residue at the end of the equilibrium solubility and dissolution experiments are shown in Fig. S5. In summary, the solubility of SACT is modulated by forming cocrystals with CAF, INIC and THEO. SACT−CAF cocrystal showed lower solubility and good stability by in vitro experiments.

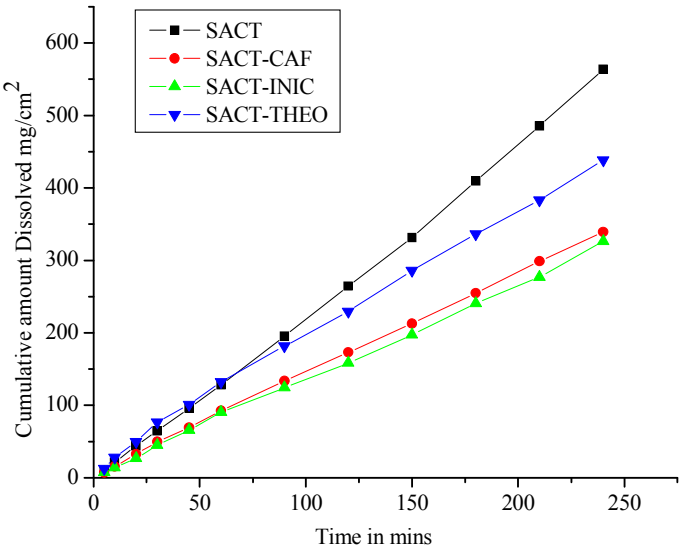

Fig. 8 Intrinsic dissolution rate curves of SACT cocrystals in pH 7 phosphate buffer.

Table 4 Intrinsic dissolution rate curves of SACT cocrystals along with $AUC_{0\text{-}4h}$ values, melting point of cocrystals and solubility of coformers.

Compound	Eq. Solubility (g/L)	IDR in ($mg/cm^2/min$)[a]	M.P (°C) of cocrystals
SACT	12.5	2.18	–
SACT-CAF	8.64 (x 0.69)	1.49 (x 0.68)	179-181
SACT-INIC	–	1.39 (x 0.64)	119-121
SACT-THEO	–	2.18 (x 1)	169-171

[a] The value in parenthesis is factor compared to the pure drug.

Conclusions

The primary aim of this study was to lower the solubility of SACT which in turn was hypothesized to modify its half life and improve drug residence time. Even though several research groups have studied different drug delivery strategies to address this issue, the cocrystallization method is unique to our study. A solid form screen of SACT resulted in cocrystals with CAF, INIC, THEO and BIP in addition to a salt with 4AP. Solubility measurements in pH 7 phosphate buffer media showed that SACT−CAF cocrystal has low solubility (0.69 times that of drug) and is stable for 24 h in the buffer slurry medium. Dissolution experiments in the same media showed that SACT−INIC and SACT−CAF have 0.64 and 0.68 times the IDR that of SACT. The low solubility and good stability of SACT−CAF cocrystal may be useful in addressing the poor residence time and faster elimination issues of SACT similar to extended release formulations.

Acknowledgements

AN thanks the DST (JC Bose Fellowship SR/S2/JCB-06/2009), CSIR (Pharmaceutical Cocrystals Project 01/2410)/10/EMR-II), and DST-SERB (Novel Solid-state Forms of APIs, SR/S1/OC-37/2011) for research funding. DST (IRPHA) and UGC (PURSE grant) are thanked for providing instrumentation and infrastructure facilities at UoH. N.R.G. and R.A.K. thank the CSIR and UGC for fellowship.

References

1. C. A. Hull and S. M. Johnson, *Cutis*, 2004, **73**, 425.
2. (a) J. Q. Del Rosso, *Cutis,* 2004, **73**, 29; (b) I. Meghan, B. S. Dubina, B. Alan and M. D. Fleischer Jr., *Arch. Dermatol.,* 2009, **145**, 1027.
3. A. Mastrolorenzo and C. T. Supuran, *Met. Based Drugs*, 2000, **7**, 49.
4. http://www.drugbank.ca/drugs/DB00634 (accessed on 13th Jan. 2014).
5. (a) D. Sensoy, E. Cevher, A. Sarici, M. Yilmaz, A. Özdamar and N. Bergisadi, *Eur. J. Pharm. Biopharm.,* 2009, **72**, 487-495; (b) B. Mandal, K. S. Alexander, A. T. Riga, *J. Pharm. Pharmaceut. Sci.,* 2010, **13**, 510.
6. *Remington: The Science and Practice of Pharmacy*, Ed. D. B. Troy, 21st ed., Lippincott Williams and Wilkins, New York, 2006, p. 907.
7. (a) N. Schultheiss and A. Newman, *Cryst. Growth Des.,* 2009, **9**, 2950; (b) W. Jones, W. D. S. Motherwell and A. V. Trask, *MRS Bulletin*, 2006, **31**, 875; (c) P. Vishweshwar, J. A. McMahon, J. A. Bis and M. J. Zaworotko, *J. Pharm. Sci*., 2006, **95**, 499; (d) N.R. Goud, S. Gangavaram, K. Suresh, S. Pal, S. G. Manjunatha, S. Nambiar and A. Nangia, *J. Pharm. Sci.,* 2012, **101**, 664.
8. http://www.fda.gov/Food/IngredientsPackagingLabeling/GRAS/ (accessed 13th Jan. 2014).
9. (a) M. Ghosh, A. K. Basak and S. K. Mazumdar, *J. Crystallogr. Spectrosc. Res*., 1987, **17**, 739; (b) M. Ghosh, A. K. Basak and S. K. Mazumdar, *Acta Crystallogr., Sect. C: Cryst. Struct. Commun.,* 1990, **46**, 1223; (c) P. A. M. Leger, S. Alberola and E. A. Karpy, *Acta Crystallogr., Sect. B: Struct Crystallogr. Cryst. Chem.,* 1977, **33**, 1455; (d) N. R. Goud and A. Nangia, *CrystEngComm*, 2013, **15**, 7456; (e) The crystal structures may be viewed in Cambridge Crystallographic Data Centre, UK, www.ccdc.cam.ac.uk (accessed 13th Jan. 2014).
10. (a) N. G. Das and S. K. Das, *Formulation Fill and Finish*, 2003, p. 10; (b) P. M. Brooks, M. S. Roberts and B. Patel, *Br. J. Clin. Pharmacol.,* 1978, **5**, 337.
11. A. J. Smith, P. Kavuru, K. K. Arora, S. Kesani, J. Tan, M. J. Zaworotko and R. D. Shytle, *Mol. Pharmaceutics*, 2013, **10**, 2948.
12. T. Higuchi and I. H. Pitman, *J. Pharm. Sci*., 1973, **62**, 55.
13. (a) A. V. Trask and W. Jones, *Top Cur. Chem*., 2005, **254**, 41; (b) N. Shan, F. Toda and W. Jones, *Chem Commun.,* 2002, **20**, 2372.

14. (a) *SAINT-Plus*, version 6.45; Bruker AXS Inc.: Madison, WI, 2003; (b) G. M. Sheldrick, *SADABS*, Program for Empirical Absorption Correction of Area Detector Data, University of Göttingen, Germany, 1997; (c) *SMART (Version 5.625) and SHELX-TL (Version 6.12)*; Bruker-AXS Inc.: Madison, WI, 2000; (d) G. M. Sheldrick, *SHELXS-97and SHELXL-97*; University of Göttingen, Germany, 1997; (e) CrysAlis CCD and CrysAlis RED, Versions 1.171.33.55, Oxford Diffraction, Oxford, 2008; (f) O. V. Dolomanov, L. J. Bourhis, R. J. Gildea, J. A. K. Howard and H. Puschmann, *J. Appl. Crystallogr.,* 2009, **42**, 339; (g) A. L. Spek, PLATON: *A Multipurpose Crystallographic Tool*; Utrecht University: Utrecht, The Netherlands, 2002; (h) L. J. Barbour, *Supramol. Chem*., 2001, **1**, 189; (i) L. J. Barbour, *X-Seed, Graphical Interface to SHELX-97 and POV-Ray;* University of Missouri-Columbia: Columbus, MO, 1999.
15. T. Higuchi and K. A. Connors, *Adv. Anal. Chem. Instrum*., 1965, **4**, 117.
16. (a) G. R. Desiraju, *Angew. Chem. Int. Ed. Engl.,* 1995, **34**, 2311; (b) R. D. B. Walsh, M. W. Bradner, S. Fleischman, L. A. Morales, B. Moulton, N. Rodriguez-Hornedo and M. J. Zaworotko, *Chem Commun*., 2003, 186.
17. (a) M. C. Etter, *Acc. Chem. Res*., 1990, **23**, 120; (b) M. C. Etter, *J. Phys. Chem.*, 1991, **95**, 4601.
18. (a) A. Nangia and G. R. Desiraju, *Top Curr. Chem*., 1998, **198**, 57; (b) P. Vishweshwar, A. Nangia and V. M. Lynch, *Cryst. Growth Des*., 2003, **3**, 783; (c) N. J. Babu, L. S. Reddy and A. Nangia, *Mol. Pharmaceutics*, 2007, **4**, 417; (d) L. S. Reddy, N. J. Babu and A. Nangia, *Chem Commun*, 2006, 1369.
19. (a) T. Steiner, *Acta Crystallogr., Structural Science*, *Sect. B*, 2001, **57**, 103; (b) J. A. McMahon, J. A. Bis, P. Vishweshwar, T. R. Shattock, O. L. McLaughlin and M. J. Zaworotko, *Z. Kristallogr.*, 2005, **220**, 340; (c) F. H. Allen, W. D. S. Motherwell, P. R. Raithby, G. P. Shields and R. Taylor, *New J. Chem*., 1999, 25; (d) A. Nangia, *J. Chem. Sci.*, 2010, **122**, 295.
20. B. P. V. Eijck and J. Kroon, *Acta Crystallogr., Structural Science , Sect. B*, 2000, **56**, 535.
21. J. Bernstein, R. E. Davis, L. Shimoni and N. L. Chang, *Angew. Chem. Int. Ed. Engl.*, 1995, **34**, 1555.
22. (a) C. B. Aakeroy, M. E. Fasulo and J. Desper, *Mol. Pharmaceutics*, 2007, **4**, 317; (b) B. Sarma, N. K. Nath, B. R. Bhogala and A. Nangia, *Cryst. Growth Des*., 2009, **9**, 1546; (c) S. L. Childs, G. P. Stahly and A Park, *Mol. Pharmaceutics,* 2007, **4**, 323; (d) A. J. Cruz-Cabeza, *CrystEngComm,* 2012, **14**, 6362.
23. (a) W Jones, W. D. S. Motherwell and A. V. Trask, *MRS Bull.,* 2006, **31**, 875; (b) M. K. Stanton and A. Bak, *Cryst. Growth Des*., 2008, **8**, 3856; (c) M. K. Stanton, S. Tufekcic, C. Morgan and A. Bak, *Cryst. Growth Des*., 2009, **9**, 1344.
24. T. Ahmad, *Pharmazie*, 1982, **37**, 559.
25. (a) K. D. M. Harris, M. Tremayne and B. M. Kariuki, *Angew. Chem. Int. Ed*., 2001, **40**, 1626; (b) K. D. M. Harris, M. Tremayne, P. Lightfoot and P. G. Bruce, *J. Am. Chem.*

Soc., 1994, **116**, 3543; (c) E. Y. Cheung, S. J. Kitchin, K. D. M. Harris, Y. Imai, N. Tajima and R. Kuroda, *J. Am. Chem. Soc.,* 2003, **125**, 14658.

26. (a) R. M. Silverstein, *Spectrometric Identification of Organic Compounds*, 6th Ed.; John Wiley & Sons, Inc.: New York, 2002; (b) E. Smith and G. Dent, *Modern Raman Spectroscopy, A Practical Approach*, John Wiley: New York, 2005.
27. (a) F. G. Vogt, J. S. Clawson, M. Strohmeier, A. J. Edwards, T. N. Pham and S. A. Watson, *Cryst. Growth Des.,* 2009, **9**, 921; (b) D. Braga, L. Maini, G. de Sanctis, K. Rubini, F. Grepioni, M. R. Chierotti and R. Gobetto, *Chem – Eur. J*., 2003, **9**, 5538.
28. L. X. Yu, A. S. Carlin, G. L. Amidon and A. S. Hussain, *Int. J. Pharm*., 2004, **270**, 221.
29. (a) S. L. Childs, L. J. Chyall, J. T. Dunlap, V. N. Smolenskaya, B. C. Stahly and G. P. Stahly, *J. Am. Chem. Soc*., 2004, **126**, 13335-13342; (b) C. B. Aakeroy, S. Forbes and J. Desper, *J. Am. Chem. Soc*., 2009, **131**, 17048-17049.

Table of Contents

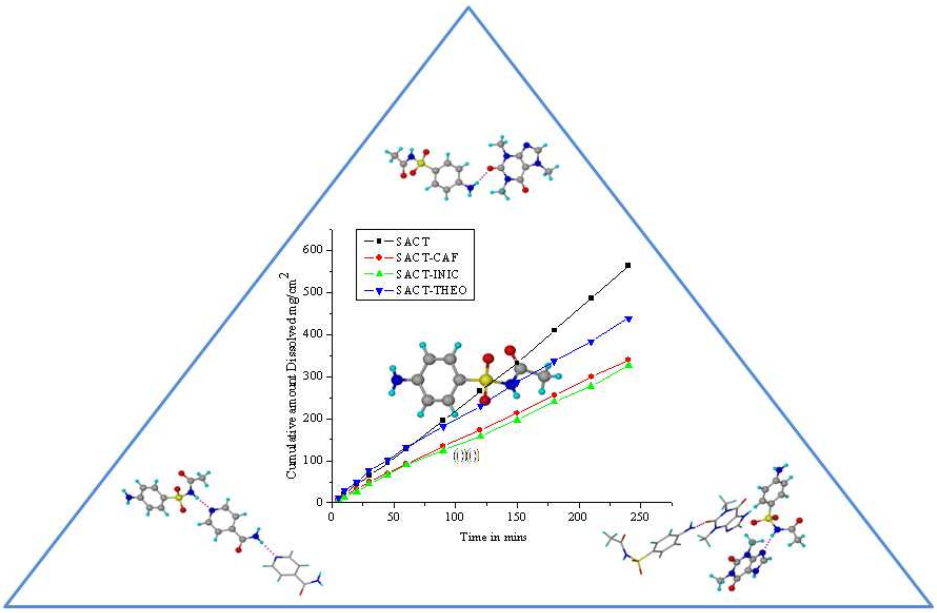

The antibacterial drug sulfacetamide was screened with pharmaceutically acceptable coformers to discover solid forms with low solubility. Cocrystals with INIC and CAF exhibited 0.64 and 0.68 times the IDR of parent drug. SACT–CAF cocrystal with lower solubility and good stability is a potential candidate to increase the drug residence time at the site of action for improved therapeutic efficacy.